Deposition of Amorphous Hydrogenated Carbon Nitride Films with a Dielectric Barrier Discharge

ARTICLE *in* PLASMA PROCESSES AND POLYMERS · JULY 2012

Impact Factor: 2.45 · DOI: 10.1002/ppap.201100185

4 AUTHORS:

Ulrike Martens
University of Greifswald
8 PUBLICATIONS **8** CITATIONS
SEE PROFILE

Thejaswini H C
Portland State University
7 PUBLICATIONS **28** CITATIONS
SEE PROFILE

Abhijit Majumdar
Indian Institute of Engineering Science and …
33 PUBLICATIONS **312** CITATIONS
SEE PROFILE

Rainer Hippler
University of Greifswald
331 PUBLICATIONS **3,411** CITATIONS
SEE PROFILE

Deposition of Amorphous Hydrogenated Carbon Nitride Films with a Dielectric Barrier Discharge

Ulrike Martens, H. C. Thejaswini, Abhijit Majumdar, Rainer Hippler*

Thin amorphous carbon nitride (CN_x) films have been deposited by DBD plasma. Deposition experiments have been performed on flat silicon (100) substrates using a C_2H_6/N_2 gas mixture and deposition times of up to 6 h. The C_2H_6/N_2 gas ratio has been varied between 1:1 and 1:5 to observe the influence of the feeding gas mixture on the chemical composition of the deposited films. The experiments were performed at gas pressures of 300 and 500 mbar. The chemical composition and bond structure of the deposited CN_x films were evaluated by X-ray photoelectron spectroscopy and by attenuated total reflectance-Fourier transform infrared spectrometry. The results show that the chemical composition of amorphous CN_x thin films depends on the working gas composition. Films deposited with higher nitrogen gas concentrations show a larger N/C ratio, an increase of C=N and C≡N bonds, and become harder.

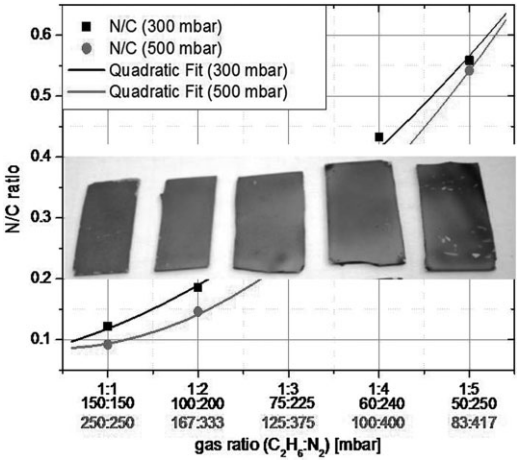

1. Introduction

Carbon nitride (CN_x) films have attracted great interest for industrial applications because of their mechanical characteristics of hardness, elasticity, and stability. Theoretical calculations show that CN_x films can be as hard as diamond.[1] Therefore, a broad range of applications exists, for example, as protective layers against corrosion and diffusion.

Here, we report the synthesis of amorphous hydrogenated CN_x films in a dielectric barrier discharge (DBD). As an advantage, barrier discharges produce highly non-thermal low-temperature plasmas at atmospheric pressures and moderate gas temperatures in a controllable way.

U. Martens, H. C. Thejaswini, A. Majumdar, Dr. R. Hippler
Institut für Physik, Ernst-Moritz-Arndt-Universität Greifswald,
Felix-Hausdorff-Str. 6, 17489 Greifswald, Germany
E-mail: hippler@physik.uni-greifswald.de

2. Experimental Section

The experimental set-up is shown in Figure 1. The plasma chamber is made of stainless steel. The inner dimensions of the chamber are 12.3 cm in height, 18.0 cm in length, and 15.0 cm in width, yielding a chamber volume of 3 320 cm^3. The two electrodes (Figure 2) inside the chamber are made from stainless steel plates with a length of 8.3 cm, width 3.3 cm, and thickness 0.15 cm. Both stainless steel electrodes are covered by dielectrics: the upper (powered) electrode is covered with aluminum oxide ($\varepsilon \approx 10$) and the lower (grounded) electrode with a glass plate ($\varepsilon \approx 3.8$). Both electrodes are separated 0.2 cm from each other by a Teflon (PTFE) spacer with

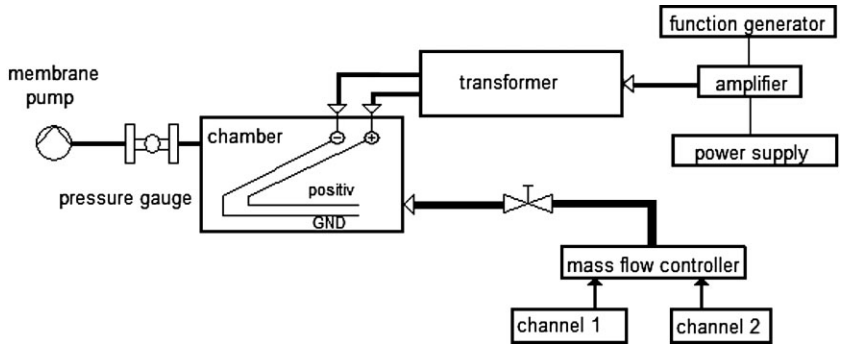

Figure 1. Experimental set-up (schematic).

symmetrically arranged holes. While the lower electrode is grounded, the upper electrode is connected to a home-built high voltage power supply. The high voltage power supply consists of a frequency generator delivering a sinusoidal output that is fed into an audio amplifier. The amplifier can be operated at up to 500 W; its output is fed into a spark plug transformer. Experiments were performed at 5 kHz.[2]

The chamber is pumped by a membrane pump down to about 10 mbar. The experiments were performed at pressures of 300 and 500 mbar. Pressure inside the plasma chamber was controlled by two gas flow controllers for ethane (C_2H_6) and nitrogen (N_2) and by an adjustable needle valve between the chamber and the membrane pump. The electrical power was measured by placing a probe capacitor (10 nF) between the lower electrode and ground measuring the collected charge together with the applied voltage as function of time, as described by Sonnenfeld et al.[3] and Wagner et al.[4] The discharge power is calculated from the resulting Lissajous figure displayed by a digital oscilloscope. For the chosen chamber pressures of 300 and 500 mbar the electrical power was set to ≈ 4 and ≈ 10 W, respectively. A higher power was required at the higher pressure in order to achieve a stable plasma operation.

Deposited films were analyzed by X-ray photoelectron spectroscopy (XPS) and by attenuated total reflectance-Fourier transform infrared (ATR-FTIR) spectrometry.

The elemental composition of the generated films was measured by XPS. The technique is able to detect all elements except hydrogen. We used a magnesium Kα anode (1 253.6 eV) as X-ray source and an hemispherical electron analyzer (CLAM2, VG Microtech). The XPS measurements were performed at a chamber pressure of 10^{-8} mbar and with pass energy of 23.5 eV at 0.125 eV · step^{-1}. The scans had a range of 200–600 eV binding energy. At first an overview spectra was created and afterwards detailed scans for different regions (carbon and nitrogen peaks) were done.

The chemical compositions of the generated films were further investigated by ATR-FTIR using a Perkin Elmer-Spectrum 65 spectrometer with a resolution of 4 cm^{-1} with a typical averaging over four scans. The absorbance was measured in reflection mode in the range of 4 000–1 000 cm^{-1}. The used ATR unit includes a diamond crystal with one reflection.

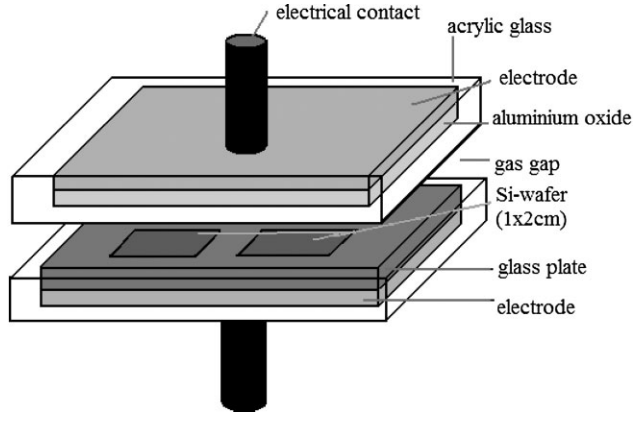

Figure 2. Electrode configuration (schematic).

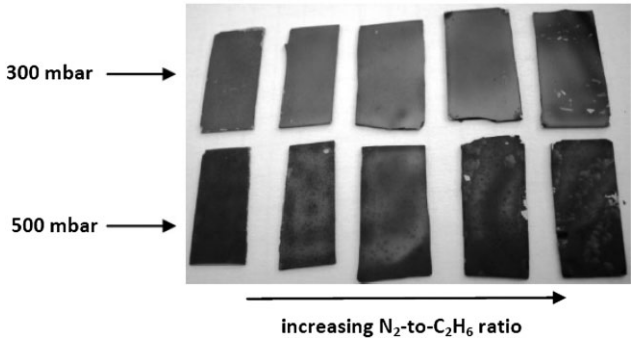

Figure 3. Photographs of the generated films deposited on silicon substrates in order of increasing nitrogen-concentration (upper series: chamber pressure 300 mbar, lower series: chamber pressure 500 mbar).

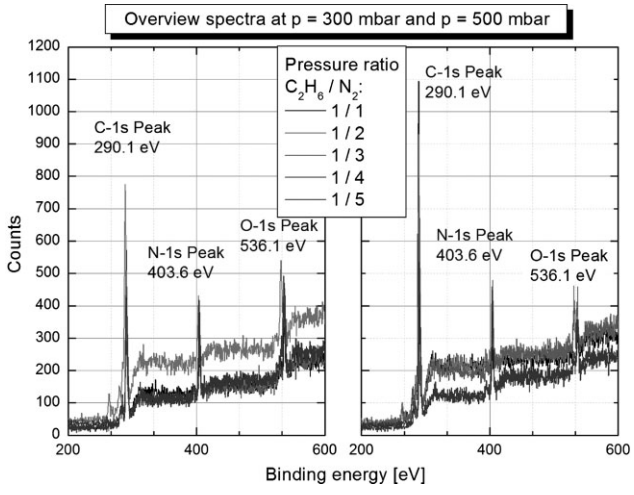

Figure 4. Overview spectra of the films generated at a pressure of (a) 300 mbar and (b) 500 mbar.

DOI: 10.1002/ppap.201100185

3. Results and Discussion

Photographs of the generated films deposited on silicon substrates are shown in Figure 3. The films show a yellow-brown color. The films generated at a chamber pressure of 300 mbar are thinner than the films generated at a pressure of 500 mbar, presumably due to the lower plasma power. At low nitrogen concentration the films become sticky and partly transparent such that the surface of the silicon substrates is partly shining through. With increasing nitrogen concentration the generated films become darker and harder with a tendency to separate from the substrate surface.

4. X-Ray Photoelectron Spectroscopy (XPS) Analysis

The elemental composition of the generated films is obtained from the XPS analysis (Figure 4). The films contain carbon (C-1s peak with a binding energy of 290.1 eV), nitrogen (N-1s peak with a binding energy of 403.6 eV), and oxygen (O-1s with a binding energy of 536.1 eV).[5,6] The oxygen composition arises from oxidation in air and depends on the post-deposition storage time. No silicon peak is observed in the spectra indicating that the deposited films are sufficiently thick. The investigated C-1s and N-1s spectra display a chemical shift that is caused by an anomalous behavior of the surface charge distribution of the silicon substrate covered by CN_x film,[6] Taking Si (2p) with a binding energy of 99.3 eV as a reference the shift was quantified. The results presented here have been corrected by subtracting the observed shift (4.5 ± 0.5 eV) for all analyses.

The different regions of carbon and nitrogen were separately scanned for more detailed information. Figure 5a and b shows the C-1s peak for different gas compositions. With increasing N_2-to-C_2H_6 gas ratio the C-1s intensity reduces, the peak becomes broader, more asymmetric, and slightly shifts to larger binding energies. It reflects the lower carbon and larger nitrogen concentration in the film. Conversely, the intensity of the N-1s peak increases (Figure 5c and d) with increasing N_2-to-C_2H_6 gas ratio. Due to the formation of CN bonds carbon is becoming more inhomogeneous with the increase of nitrogen concentration. Also a shift of the C-1s peak appears due to the presence of hydrogenated CN_x groups. The position of the N-1s peak centered at ≈399 eV is an indication for the formation of C–NH_x species. Tabbal et al.[10] proposed that due to the presence of C–NH_x species the N-1s peak is centered at 399.4 eV, while unhydrogenated C–N would have a peak around 398.5 eV. Taking the atomic sensitive factor (ASF) into account the N/C ratio in the film was evaluated. The measured N/C ratio (Figure 6) shows an approximately quadratic increase from about 0.1 (1:1) to 0.55 (1:5) with the N_2-to-C_2H_6 ratio in the working gas. No justification for this dependency can be given yet.

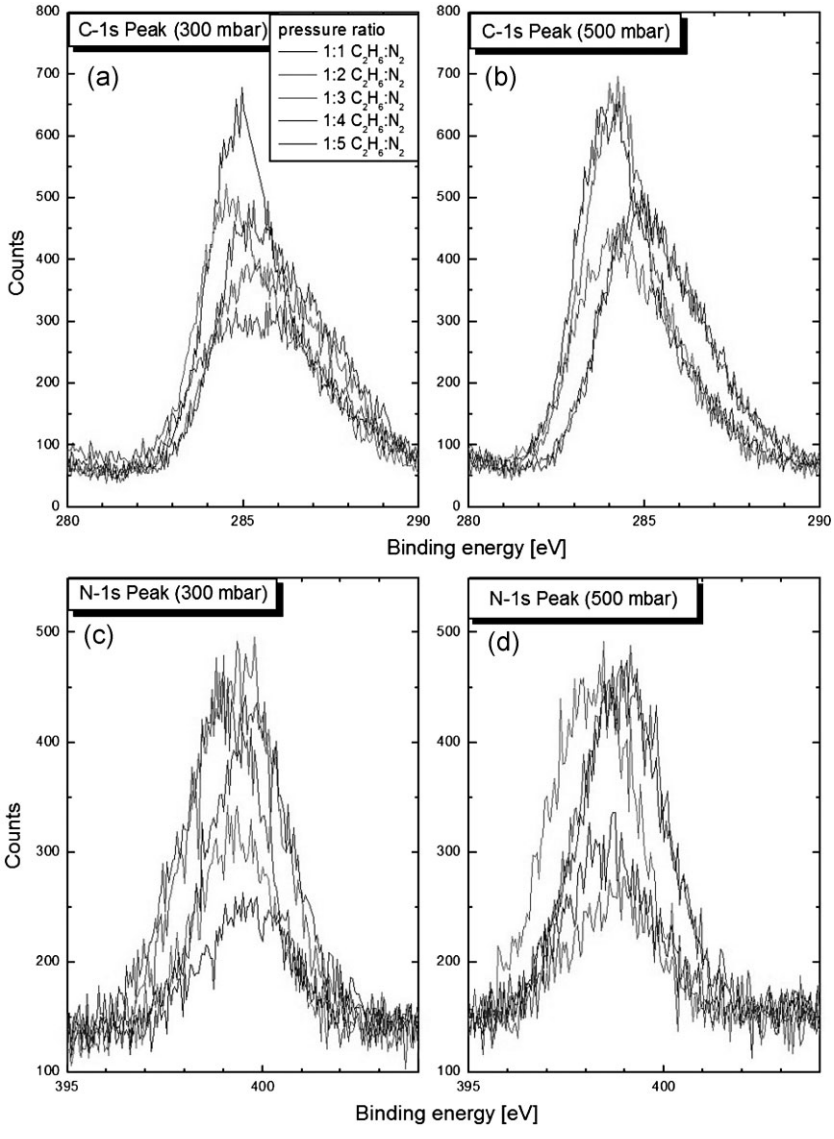

Figure 5. High resolution scans of C-1s (a and b) and N-1s (c and d) peaks for different pressures (300 and 500 mbar) and gas ratios.

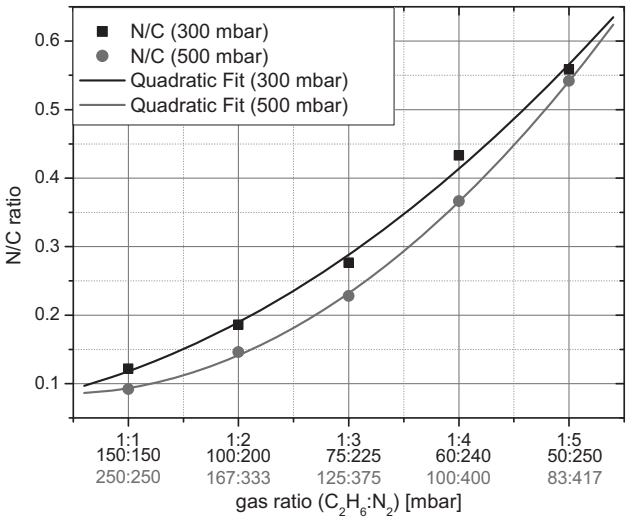

Figure 6. Nitrogen/carbon (N/C) ratio in the deposited films in dependence on the gas ratio.

5. ATR-FTIR

For the FTIR absorption measurements we used the powders generated by scratching the films off the electrodes. The analyses were made for powders generated at a chamber pressure of 500 mbar and C_2H_6:N_2 gas ratios of 1:2, 1:3, 1:4 and 1:5. The results are displayed in Figure 7.

5.1. Assignment of the IR Bands

In all FTIR spectra a band at 2 180 cm^{-1} of triple-bonded nitrogen with carbon (C≡N, nitrile group) and triple bonded C≡C was observed (Table 1). This band becomes more intense with larger nitrogen gas concentrations. Similarly, bands of

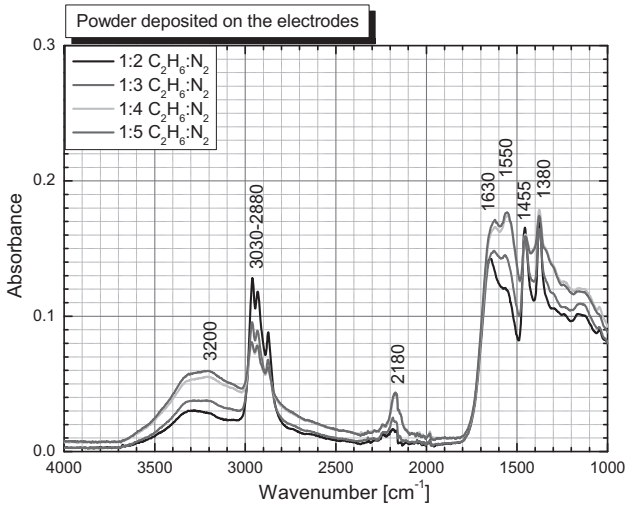

Figure 7. FTIR-ATR absorption spectra of powders generated from the films deposited on the electrodes at C_2H_6:N_2 gas ratios of 1:2, 1:3, 1:4 and 1:5 (chamber pressure 500 mbar).

double-bonded C=N at 1 550 cm^{-1} and single bonded carbon with nitrogen (C–N) in the range of 1 380 cm^{-1} occur. All the three bands show the same characteristics in dependency on the relative nitrogen gas concentration.

The bands in the range of 1 750–1 500 cm^{-1} can be assigned to vibrations of C=C bonds, C=N bonds, and C–N bonds. In the range of 1 090–1 020 cm^{-1} the C–N stretching absorption of primary aliphatic amines appears. The band centered at 1 150 cm^{-1} is related to C–C skeletal vibrations.

In the 3 600–3 200 cm^{-1} range a band of N–H stretching vibrations can be observed. With higher nitrogen gas concentration this band increases. The same holds for the N–H bending vibrations which appear at 1 630 cm^{-1}. The band centered at 3 200 cm^{-1} overlaps with the stretching vibration of OH groups. It is complicated to separate the overlapping bands. As a result a pronounced and rather broad band is observable in Figure 7.

In the 3 030–2 800 cm^{-1} range three characteristic absorption bands appear due to asymmetric and symmetric C–H stretching vibrations in aliphatic CH, CH_2 and CH_3. The asymmetric stretching vibration of CH_3 is located at 2 975–2 950 cm^{-1}. Next to that band the absorption band of CH_2 occurs at about 2 930 cm^{-1}. The third peak in that range seems to be an overlapping symmetric stretching band of CH_3 located at 2 885–2 865 cm^{-1} and CH_2 at 2 870–2 840 cm^{-1}.

The absorption band detected at 1 455 cm^{-1} is attributed to the asymmetric deformation of methyl groups in hydrocarbons. In the range of 1 380 cm^{-1} the symmetric absorption band can be observed. The intensity of these bands decreases with lower gas concentration of C_2H_6.

It is notable from Figure 7 that the composition of the band intensities changes with higher nitrogen concentrations in the film. With an increase of nitrogen the intensity of the C≡N band is increasing while the CH_x bands show a decreasing trend. It was argued by Majumdar et al.[6] that

Table 1. Assignment of observed infrared bands.

Band (cm^{-1})	Assignment	References
3 200	NH stretching	[10,12–15]
	OH stretching	
3 030–2 800	CH stretching	[8,9,12,13,15]
2 180	C≡N stretching	[7,8,13–15]
	C≡C stretching	
1 750–1 500	C–N stretching	[8,11,14,15]
	C=C stretching	
1 630	N–H deformation	[7,13]
1 550	C=N stretching	[8,10,11,13]
1 455	CH_x def. asym.	[10,13,15]
1 380	CH_x def. sym.	[13,15]
1 260–1 000	C–C stretching	[13]

DOI: 10.1002/ppap.201100185

nitrogen due to its larger electronegativity interacts with ethane and forms nitrile/isonitrile groups resulting in a decrease of CH_x. The FTIR-ATR spectra (Figure 7) also show that the films with larger N/C ratio contain more C=N and C≡N bonds.

The plasma and chemical reactions contributing to film growth and to film composition are electron impact-induced fragmentation of C_2H_6 and N_2 precursor molecules into smaller molecules and radicals, for example, CH_2, CH_3, C_2H_3, C_2H_4, C_2H_5 and N. The radicals are highly reactive and, already in the gas, can form larger molecules which further react in the gas phase or condense on the growing film.[16] Reactions of nitrogen atoms with small hydrocarbon molecules are of particular importance,[17,18] for example

$$N + CH_2 \rightarrow HCN + H$$

and

$$N + CH_3 \rightarrow H_2CN + H$$

as they contribute to the formation of carbon and nitrogen-containing molecules.[18]

6. Conclusion

Amorphous CN_x films were deposited in a C_2H_6/N_2 gas mixture with the help of DBD. The chemical composition of amorphous CN_x thin films depends on the working gas composition. Films deposited with higher nitrogen gas concentrations show a larger N/C ratio of up to 0.55 and become harder. The bond structure was investigated by FTIR and several double (C=N) and triple bonds (C≡N and C≡C) were identified.

Acknowledgements: The work was supported by the Deutsche Forschungsgemeinschaft (DFG) through SFB/TR 24 *Complex Plasmas*.

Received: October 13, 2011; Revised: December 22, 2011; Accepted: January 16, 2012; DOI: 10.1002/ppap.201100185

Keywords: ATR-FTIR; dielectric barrier discharge (DBD); ESCA/XPS; hydrocarbons; thin film deposition

[1] A. Y. Liu, M. L. Cohen, *Science* **1989**, *245*, 841.
[2] A. Majumdar, J. F. Behnke, R. Hippler, K. Matyash, R. Schneider, *J. Phys. Chem. A* **2005**, *109*, 9371.
[3] A. Sonnenfeld, T. M. Tun, K. V. Kozlov, H.-E. Wagner, J. F. Behnke, R. Hippler, *Plasma Polym.* **2002**, *6*, 237.
[4] H.-E. Wagner, R. Brandenburg, K. V. Kozlov, A. Sonnenfeld, P. Michel, J. F. Behnke, *Vacuum* **2003**, *71*, 417.
[5] J. F. Moulder, W. F. Stickle, P. E. Sobol, K. D. Bomben, *Handbook of X-Ray Photoelectron Spectroscopy*, Perkin-Elmer Corporation, Eden Prairie **1979**.
[6] A. Majumdar, G. Das, K. R. Basvani, J. Heinicke, R. Hippler, *J. Phys. Chem. B* **2009**, *113*, 15734.
[7] H.-X. Han, B. J. Feldman, *Solid State Commun.* **1988**, *65*, 921.
[8] A. Zocco, A. Perrone, A. Luches, R. Rella, A. Klini, I. Zergioti, C. Fotakis, *Thin Solid Films* **1999**, *349*, 100.
[9] C. Moreno Castilla, M. A. Ferro-Garcia, J. P. Joly, I. Bautista-Toledo, F. Carrasco-Marin, J. Rivera-Utrilla, *Langmuir* **1995**, *11*, 4386.
[10] M. Tabbal, P. Merel, S. Moisa, M. Chaker, E. Gat, A. Ricard, M. Moisan, S. Gujrathi, *Surf. Coat. Technol.* **1998**, *98*, 1092.
[11] X.-A. Zhao, C. W. Ong, Y. C. Tsang, Y. W. Wong, P. W. Chan, C. L. Choy, *Appl. Phys. Lett.* **1995**, *66*, 2652.
[12] C. Y. Tang, Y.-N. Kwon, J. O. Leckie, *J. Membr. Sci.* **2007**, *287*, 146.
[13] G. Socrates, *Infrared Characteristic Group Frequencies*, 2nd edition, John Wiley & Sons, Chichester **1994**.
[14] Y. Yin, K. Fisher, N. J. Nosworthy, D. Bax, S. Rubanov, B. Gong, A. S. Weiss, D. R. McKenzie, M. M. M. Bilek, *Plasma Polym.* **2009**, *6*, 658.
[15] J. Kim, D. Jung, Y. Park, Y. Kim, D. W. Moon, T. G. Lee, *Appl. Surf. Sci.* **2007**, *253*, 4112.
[16] H. C. Thejaswini, A. Majumdar, T. M. Tun, R. Hippler, *Adv. Space Res.* **2011**, *48*, 857.
[17] C. D. Pintassilgo, J. Loureiro, *Planet. Space Sci.* **2009**, *57*, 1621.
[18] G. Horvath, F. Krema, L. Polachova, K. Klohnova, N. J. Mason, M. Zahoran, S. Matejcik, *Eur. Phys. J. Appl. Phys.* **2011**, *53*, 11001.